

# Scanning Tunneling Spectroscopy in MgB<sub>2</sub>

P. Martinez-Samper, J.G. Rodrigo, G. Rubio-Bollinger, H. Suderow, S. Vieira<sup>a</sup>  
S. Lee, S. Tajima<sup>b</sup>

<sup>a</sup>*Laboratorio de Bajas Temperaturas, Depto. Fisica de la Materia Condensada, Instituto de Ciencia de Materiales N. Cabrera, Universidad Autonoma de Madrid, E-28049 Madrid, Spain\**

<sup>b</sup>*Superconductivity Research Laboratory, ISTEK, 1-10-13, Shinonome, Koto-ku, Tokyo, 135-0062 Japan*

---

## Abstract

We present extensive Scanning Tunneling Spectroscopy (STM/S) measurements at low temperatures in the multi-band superconductor MgB<sub>2</sub>. We find a similar behavior in single crystalline samples and in single grains, which clearly shows the partial superconducting density of states of both the  $\pi$  and  $\sigma$  bands of this material. The superconducting gaps corresponding to both bands are not single valued. Instead, we find a distribution of superconducting gaps centered around 1.9mV and 7.5mV, corresponding respectively to each set of bands. Interband scattering effects, leading to a single gap structure at 4mV and a smaller critical temperature can be observed in some locations on the surface. S-S junctions formed by pieces of MgB<sub>2</sub> attached to the tip clearly show the subharmonic gap structure associated with this type of junctions. We discuss future developments and possible new effects associated with the multiband nature of superconductivity in this compound.

*Keywords:* MgB<sub>2</sub>, superconductivity, tunneling spectroscopy, local probes

---

## 1. Introduction

The surprising discovery by Nagamatsu et al.[1] of superconductivity at 40 K in the previously well known material MgB<sub>2</sub>, which is particularly simple from the structural point of view, attracted immediately the interest of many research groups in the world. Soon after its discovery, several experiments appeared in the electronic archive cond-mat, and subsequently in conventional journals,

revealing some microscopic aspects of the superconductivity in this compound that turned out later on to be essential for its understanding. The boron isotope effect, discovered by Bud'ko et al.[2] pointed towards a phonon mediated pairing interaction, and the tunneling spectroscopy, measured with a Scanning Tunneling Microscope (STM/S), showed a clean BCS density of states with an intriguing low value for the ratio  $2\Delta/k_B T_c = 1.2$  [3], as compared to the value expected from simple BCS theory (3.53). First principles investigations of the electron-phonon coupling concluded that two gaps, related to the two different sets

---

<sup>1</sup> \* Grupo Intercentros de Bajas Temperaturas, ICOMM-CSIC and LBT-UAM.

Corresponding author: sebastian.vieira@uam.es

of bands of the Fermi surface would exist in this superconductor[4], and that the gap reported in Ref.[3] could be associated to one of these sets of bands. Within another interesting approach, Bascones and Guinea [5] considered the effect of the surface as a topological defect in two band superconductors to explain the observation of a single gap structure in some early tunneling experiments[3,6,7,8].

Two band superconductivity was theoretically proposed by Suhl, Matthias and Walker in 1959[9], and has been discussed since then in relation to other materials. For instance, important tunneling experiments were made by Binnig et al. in 1980 [10] on Nb doped SrTiO<sub>3</sub>. These authors were able to measure in a very neat way the two quasiparticle peaks in the superconducting tunneling density of states due to the opening of two gaps corresponding to the two bands of the Fermi surface of this compound, filled one after the other by the Nb doping. The results were compared to reduced SrTiO<sub>3</sub>, where only a broadened single peak structure is observed, together with a four times larger residual resistivity. Interband scattering due to an increasing amount of defects or impurities is indeed expected to gradually merge multigap features in the density of states into the typical BCS single gap curve[11,12,13].

Even if first measurements of the tunneling density of states reported the observation of a single gap structure corresponding to different values of the superconducting gap (with  $2\Delta/k_B T_c$  between 3 and 4 [6,7,8]), more recent experiments [14,15,16,17,18] are in good agreement with the model proposed in [4]. Therefore, we can now state that tunneling spectroscopy experiments made in this material support well the two gap scenario. As it is well known, other very powerful macroscopic thermal and magnetic measurements, as well as microscopic spectroscopic probes, which will be treated in detail by other authors in this volume, produced more and more compelling evidence in this direction (see e.g. [19,20,21,22,23,24,25,26]).

Previously existing band structure calculations [27] were reconsidered in order to understand

the microscopic nature of the superconducting state[28,29,30]. Precise calculations based on the strong coupling formalism of Eliashberg have been recently made by the authors of Ref.[31]. It has been shown, and confirmed by comparing de Haas van Alphen experiments with the band structure calculations [32,33], that the electron phonon interaction varies strongly on the Fermi surface. Mainly four sheets are found, two of them being near cylinders due to the two dimensional antibonding states of boron  $p_{xy}$  orbitals, and two three dimensional sheets from the  $\pi$  bonding and antibonding states of the boron  $p_z$  orbitals[32,34]. The superconducting gap  $\Delta(\vec{k})$  has been calculated as a function of temperature and magnetic field and is non zero everywhere on the Fermi surface. However, its size changes strongly clustering around two main values related to the  $\sigma$  and  $\pi$  sheets[31]. The smaller value, which was measured in our first experiments [3], appears to be related to the three dimensional  $\pi$  sheets, and the larger one to the two dimensional  $\sigma$  sheets.

We can therefore affirm that today it is widely accepted that MgB<sub>2</sub> is a multiband superconductor where the basic physics can be theoretically understood in a very sound way. This opens a new and interesting challenge to improve the accuracy of the experimental results and push the theoretical developments towards more and more narrow limits. The search for new phenomena associated with two band superconductivity appears especially promising. With respect to other known multiband superconductors, as e.g. doped SrTiO<sub>3</sub>[10] or the nickel borocarbides[35], MgB<sub>2</sub> has the considerable advantage of having a high critical temperature and a relatively simple Fermi surface.

Local vacuum tunneling spectroscopy at low temperatures, made possible with the use of the STM/S, is a very promising technique, as it gives a direct measurement of the local density of states[36]. This is even more useful in the case of materials, as MgB<sub>2</sub>, where the superconducting gap is strongly  $\vec{k}$  dependent. The use of an atomically sharp counter-electrode whose (x,y,z) position can be changed at will in-situ, gives in

principle access to detailed information about the superconducting density of states in very different regions of the Fermi surface. However, to get fully reliable data we need to reduce as much as possible all pair breaking effects acting on the surface of the condensate. Careful filtering of all wires arriving to the sample turns out to be extremely important. The measured spectra most accurately approach the local superconducting density of states (LDOS) of the sample when the measurement is made near  $T=0\text{K}$  to reduce thermal smearing. Obviously, characterizing and controlling the surface of the sample is of extreme importance for a proper use of this technique.

We should remark that, although other type of spectroscopic measurements provide very useful information about the density of states, the STM/S has the advantage of being a direct probe where a very high resolution in energy can be achieved by measuring at sufficiently low temperatures. For example, photoemission spectroscopy also gives a direct measurement of the density of states in different parts of the Fermi surface, but present experiments [26] have much less resolution in energy than STM/S. Point contact spectroscopy has been widely used in the case of  $\text{MgB}_2$  (see e.g. [19,20]), and it is also a very powerful, but less direct probe of the density of states.

Recently, small single crystals of  $\text{MgB}_2$  have been grown in a few laboratories[37,38,39], and some results on tunneling spectroscopy have been reported[18]. At zero magnetic field, STS in the  $c$  direction at low temperatures has been found in agreement with our early result on single grains of this material[3]. However, to get a proper fit to BCS theory a pair breaking parameter and a finite gap distribution, which both account for experimental smearing, need to be introduced[18]. The observation of a hexagonal vortex lattice is a new result, although more experiments are needed to understand the microscopic aspects of the Shubnikov phase in this multiband superconductor[18]. Other STM/S experiments at 4.2 K in oriented thin films, detailed in another contribution to this volume, have also found two gap features associ-

ated to different tunneling directions[6].

Several questions remain open which need to be addressed using low temperature STM/S. For example, given that this material is a multiband superconductor, how do the multiple gaps reflect in the tunneling characteristics at a given point on the surface? How can we extract information about the dominant gap structure in this material? How shall we deal with and identify the effect of interband scattering? For instance, would it be possible to find a region of the surface where a single gap is observed? A zero bias peak due to Andreev bound states, which could be related to complex phase relations between the Cooper pair wavefunction in the different bands, has been predicted in multiband, s-wave, superconductors[40]. Are there hints of such a peak in STS experiments? On the other hand, S-S junctions (which can sometimes be found in STM/S experiments) in conventional single gap superconductors show a series of small features in the conductance below the superconducting gap due to multiple Andreev reflection processes (subharmonic gap structure). At which voltage should we expect these features to appear in two gap superconductors? Actually, how do multiple Andreev reflections occur between two multiband superconductors?.

In this paper we present some of our STM/S research in  $\text{MgB}_2$ , made after the first results published in [3], and try to give insight into some of the above mentioned opened questions. New data show in both, single crystals and small grains, the same reproducible behavior independent of the sample preparation method. The two gap structures are identified in most typically found spectra. We also discuss some serendipitous events where a piece of  $\text{MgB}_2$  accidentally attached to the tip permits the observation of clear S-S tunneling features, including the first (to the best of our knowledge) observation of the subharmonic gap structure.

## 2. Experimental and sample preparation

All cryostats used to measure the data presented here (a  $^4\text{He}$ , a  $^3\text{He}$  and a dilution refrigerator) are equipped with similar, home built, STM set-ups and electronics which have been carefully filtered to produce a clean electromagnetic environment in the STM chamber. Measurements in Pb, Al and  $\text{NbSe}_2$  were used to test the energy resolution of all set-ups[41,42]. All STM's feature a very high mechanical stability and macroscopic in-situ positioning capabilities (x-y table) in a  $2\times 2\text{ mm}^2$  window. We have measured single crystals and small grains prepared in different ways. The single crystals were grown under pressure as described in [37] and are needle like with typical sizes of  $0.1\times 0.06\times 0.7\text{ mm}^3$  and the c axis along its long direction. Samples were introduced (following its long axis) in a small hole made on a sample holder (a flat gold surface) and glued with a small drop of conductive silver epoxy, which was previously put into the small hole. About half of the samples remained outside the hole. Once a sample was mechanically fixed to the sample holder, a small clean blade was used to cut it, and the tip was positioned (with the help of an optical microscope and the in-situ positioning capabilities of our STM) on top of the remaining freshly broken surface. The whole set-up was then cooled as fast as possible. The tunneling conditions were always good, leading to reproducible images and spectra over the whole surface. However, the topography is complex, showing a large amount of inclined small terraces at the nanoscopic scale, observed with STM and AFM, indicating that we could not find any cleaving plane. SEM images at a larger scale also showed a terraced surface. This means that the orientation of the surface at the length scale of the STM experiment is unknown and does not coincide with the breaking plane. The small grains were prepared following the procedure described in Ref.[3]. After dispersing them in an acetone bath in ultrasound, a small drop was deposited onto a flat gold surface, the liquid was evaporated at  $80^\circ\text{C}$  and the grains were pressed into the

gold surface using a small synthetic ruby. A subsequent bath in acetone and ultrasound removed the loosely fixed grains. Following this process, some of the samples were heated in a Ar atmosphere of 600mbar at  $200^\circ\text{C}$  during two hours to promote gold diffusion and improve the mechanical fixing of the grains.

We made an extensive topographical characterization of the surface at all locations where we took conductance versus bias voltage curves. However, here we report only about the most characteristic measured spectra (STS), because we cannot clearly associate the features of the spectra presented here to specific features of the surface topography.

## 3. Results and discussion

### 3.1. $\pi$ and $\sigma$ bands

In this paper we report about many experiments made in macroscopically different places of a large number of samples, prepared in different conditions. The goal is to show the behavior which, to our understanding, best reflects the intrinsic properties of this superconductor. Millions of tunneling conductance versus bias curves were measured. Most of them were taken in points with good tunneling conditions (reproducible imaging as a function of the bias voltage and work function of several tenths of eV to several eV), and the results (measured in all samples and preparation conditions) are comprised within two limiting behaviors. Before discussing them we should remark that an STM/S experiment always probes a part of the Fermi surface, depending on the particular atomic configuration of tip and sample surface[36,43]. Therefore, a multiband material as  $\text{MgB}_2$  is expected to show a wide variety of behaviors, because, depending on the location, one will probe different parts of the Fermi surface.

In Fig.1 we show the tunneling conductance obtained in a small grain and in a single crystal respectively. These curves show clearly the partial

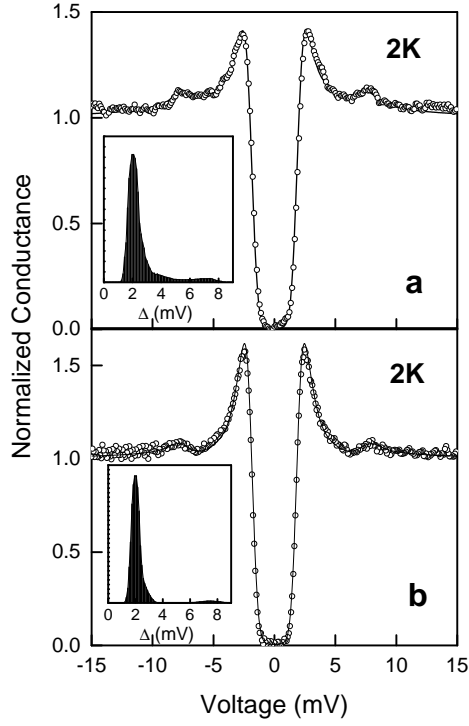


Fig. 1. Tunneling spectroscopy of MgB<sub>2</sub> at 2K (tunneling resistance  $R_N = 1M\Omega$ ), measured in a single crystal (a) and in a grain (b). The insets represent the (normalized) distribution of values of the superconducting gap used to fit the experiment according to the procedure described in the text (solid line: model, circles: experiment). At this precise location, the electrons contributing to the tunneling current come mostly from the  $\pi$  band. For clarity, a reduced number of the whole set of experimental points is plotted in this and the following figures.

density of states corresponding to the three dimensional  $\pi$  band. However, small bumps around 7.5mV can also be observed. Fig.2 shows the other limiting behavior found in our experiments, where the small bumps appearing in Fig.1 have evolved into well developed peaks. Although these spectra are clearly measured in both single crystals and grains, the curves of Fig.1 are the ones which appear most frequently on the surface of the measured MgB<sub>2</sub> samples.

From these observations we can discuss the properties of the superconducting gap in both bands. First, we should note that the density of states within the smallest superconducting gap is always zero. This implies that the pair breaking term  $\Gamma$ [44]

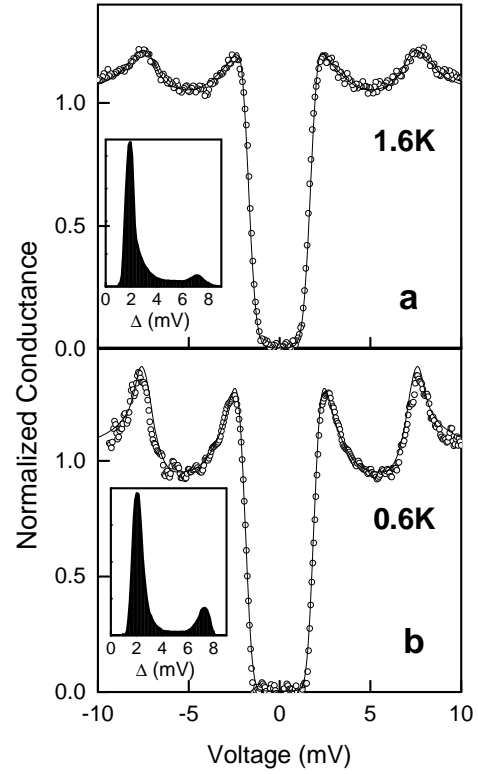


Fig. 2. Tunneling spectroscopy curves (circles) of MgB<sub>2</sub> obtained in a single crystal (a) and in a grain (b) ( $R_N = 1M\Omega$ ), together with the distribution of values of the superconducting gap used to fit the experiment (lines). At this precise location, the electrons contributing to the tunneling current come both from the  $\pi$  and  $\sigma$  bands.

is of no use to obtain an adequate fit to the experiments.

To obtain an idea of the contribution to the tunneling current from the different bands, we phenomenologically model the measured superconducting density of states by the sum over a normalized distribution of BCS densities of states corresponding to a distribution of values of the superconducting gap  $\Delta$ . As shown in Fig.1, even when we deal with the simplest and most frequent situation, i.e. a single gap structure around 1.9mV corresponding to the  $\pi$  band, a single valued gap is not enough to obtain a the best fit to the experiment. The observed quasiparticle peaks are not as high as expected from most simple s-wave BCS theory. They are smaller because of a

finite anisotropy that gives a finite distribution of values of the superconducting gap and therefore wider quasiparticle peaks. A gap distribution due to the gap anisotropy smears out the coherence peaks but the tunneling characteristics are flat-bottomed as observed in the experiments. The situation is similar to the case of the anisotropic superconductors NbSe<sub>2</sub> and the nickel borocarbide materials [45,46,47], where the tunneling characteristics taken at low temperature also show a zero density of states at low energies but broadened quasiparticle peaks.

It is immediately apparent from our results that the tunneling current comes mostly from the  $\pi$  band electrons, because the contribution to the partial density of states of the  $\sigma$  band gaps needed to explain our results is always relatively small. When its intensity increases the contribution to the tunneling current from electrons with  $\vec{k}$  vectors perpendicular to the  $c$  axis is also increasing.

Although our curves clearly indicate that the superconducting gap is not single valued in both the  $\pi$  and  $\sigma$  bands, we must emphasize that the phenomenological model used to fit the curves here gives a very qualitative idea of the different contributions to the tunneling current found in each location. Therefore, the curves shown in the insets of Figs.1,2,3 and 5 are given to illustrate the different behaviors found in different locations, but they definitely do not give the actual distribution of values of the superconducting gap corresponding to each band measured in these locations. For instance, we believe that the filling of region between the  $\pi$  and  $\sigma$  band gaps in our approach is due to interband scattering effects.

### 3.2. Interband scattering effects

As a matter of fact, it is difficult to understand in simple terms the very robust superconducting properties within the two gap model [13]. Indeed, multiband superconductivity is expected to be sensitive to non magnetic defects or impurities, as they allow for interband transitions,

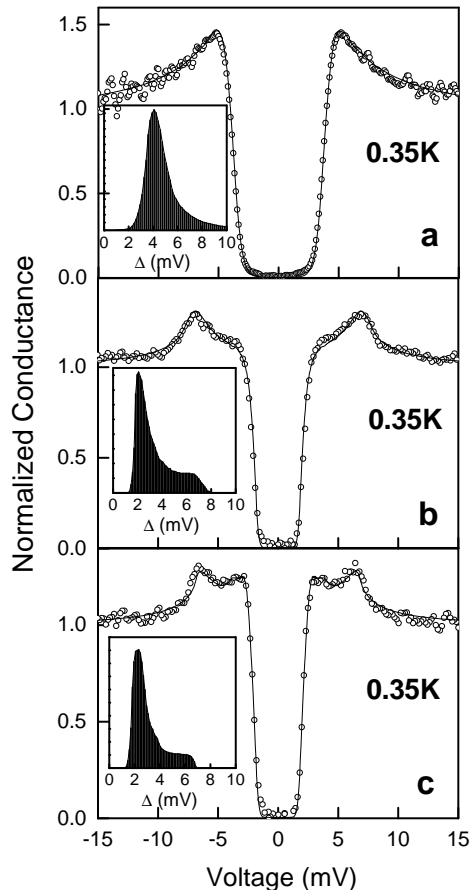


Fig. 3. Different spectra taken at different positions on a single grain (circles), and its associated fits (lines and inset). In (a) we observe a single, broadened quasiparticle peak, whereas (b) and (c) show intermediate situations between those presented in Figs. 1 and 2. We associate this behavior, which is also observed in single crystalline samples, to interband scattering effects at the surface of MgB<sub>2</sub> (see text).

increasing the smaller gap, decreasing the larger gap and leading therefore to a smaller critical temperature [11,12,13,30]. However, even bad quality samples of MgB<sub>2</sub> do not show big changes in the superconducting critical temperature, and also show both superconducting gaps with values which do not differ significantly from the best samples. The theoretical work in Ref. [13] deals with this apparent contradiction by proposing that interband scattering is particularly small in this compound. It would be highly desirable to obtain experimen-

tal evidence that changes in the superconducting density of states due to defects or impurities can indeed be observed as it is an essential ingredient of multigap superconductivity [11,12,13,30]. Recent bulk specific heat measurements [48] on irradiated samples have not been conclusive. The calculations of Ref.[5] indicate however that the surface can produce in some cases interband scattering effects that do not influence the bulk properties and which can be studied with STM/S.

We can find areas on the surface of  $\text{MgB}_2$  in which the conductance appears as shown in Fig.3a and which can be fitted with distributions of values of  $\Delta$  centered around 4mV, i.e. between  $\Delta_\pi$  and  $\Delta_\sigma$ . The superconducting features of these spectra disappear (the spectra become completely flat) around 20K. Note that the shape of this curve is in complete disagreement with possible S-S tunneling features, discussed further on and measured in Ref.[7]. We believe that this behavior (also observed in some single crystalline samples) is due to enhanced interband scattering in some regions on the surface. The value of the superconducting gap and the associated decrease in the local critical temperature agrees well with the predictions of Refs.[13,30]. Note that this is a surface effect, related to the intrinsic multigap nature of superconductivity in this compound, and which is clearly not found in bulk samples[5,48]. Similar observations have been done with STM/S in the non-magnetic nickel borocarbides, where the surface shows a very irregular topography, as in  $\text{MgB}_2$ [47]. Note that point contact experiments made in  $\text{MgB}_2$  [20] also show clearly a single gap feature with  $\Delta$  around 4mV in some measured curves, in agreement with our results and discussion. Possibly, as noted in Ref.[15], early tunnel experiments showing a smeared single gap structures around 3-4mV could be interpreted in a similar way as the spectra shown in Fig.3a.

In Figs.3b and c we show other characteristic behaviors. Within our simple phenomenological fits, the interband scattering fills the intermediate region between both bands, as shown in the insets. However, the features due to the  $\pi$  and  $\sigma$  bands

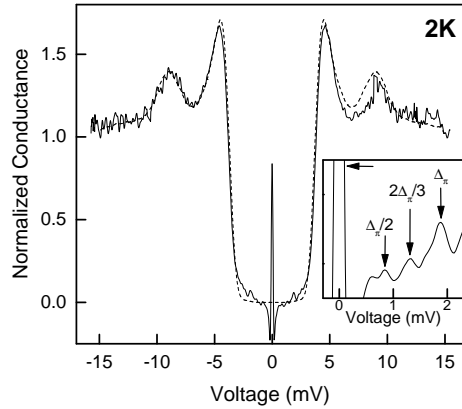


Fig. 4. Subharmonic gap structure observed in spectra characteristic for tunneling between two single grains of  $\text{MgB}_2$ , taken at 2K. The inset shows a zoom over the relevant voltage region with arrows at each peak corresponding to a submultiple of  $2\Delta_\pi$ , and at the peak originating in the conductance due the Josephson effect (arrow to the left). Note that the measured negative resistance around zero bias is a characteristic feature of junctions where the Josephson effect is observed.

are still observed.

### 3.3. S-S junctions

As described earlier, in the experiments made in single grains, we use the x-y table to change macroscopically the position of the tip with respect to the sample. This enables us to clean the tip on the gold surface and then to measure STM/S with a normal, clean gold tip on a single  $\text{MgB}_2$  grain. Sometimes however clear S-S tunneling spectra appeared, due to a loosely connected single grain which was attached by accident to the tip apex, as already mentioned in [3], where we also reported that the observed behavior was in agreement with the value of  $\Delta$  found with a clean normal tip.

In Fig.4 we represent conductance curve obtained in one of those experiments[3]. A peak in the conductance due to the Josephson current neatly appears at zero bias, and the so-called subharmonic gap structure, characteristic of S-S junctions (inset). It is indeed well known that multiple Andreev reflections occurring at the junction provide a vehicle for a finite conduction within the

superconducting gap which becomes more important when the resistance of the junction decreases (or its transparency increases; in our experiments, we always measure above  $100k\Omega$ , i.e. in the tunneling, and not in the point contact regime, see [49]). This conduction mechanism is enhanced when the bias voltage between both electrodes reaches submultiples of two times the gap value, giving sharp features in the conductance at  $2\Delta/n$  ( $n=1,2,3,\dots$ ), reminiscent of the high quasiparticle peaks of the density of states[49]. In Fig.4 we can clearly identify the dominant gap structure at  $2\Delta_\pi$  (with  $\Delta_\pi = 1.9mV$ ) and the peaks of the subharmonic gap structure at  $2\Delta_\pi/n$ , with  $n=1,2,3,4$  (higher order peaks fall below the resolution of the experiment).

On experiments in single crystals, we could also find S-S tunneling spectra (Fig.5), corresponding to accidental situations in which a loose  $MgB_2$  piece was attached to the tip. We believe that when the sample was broken before cooling the set-up, pieces in good registry with the sample were probably cleaved out. Note that the peak corresponding to a Josephson current is smaller than the one in the previously discussed junction, possibly due to differences in the Josephson coupling energy [49] (which decreases with increasing tunneling resistance  $R_N$ ;  $R_N = 500k\Omega$  in Fig.5 and  $R_N = 150k\Omega$  in Fig.4; a Josephson peak was also reported in SNS point contact junctions having a resistance of about  $30\Omega$ [50])

The conductance of this junction as a function of temperature can be fitted up to 26K to a distribution similar to the one shown in the inset of Fig.5 for the 3K curve. Note that, in agreement with Refs.[14,50], we observe a very high peak at zero bias when we increase the temperature. The combination of a large amount of thermally excited quasiparticles and a superconducting gap with a value much smaller than expected from most simple BCS theory produces these anomalous curves.

In addition to the already discussed subharmonic gap structure and the Josephson effect, two additional clear peaks appear at higher bias voltages in Figs.4 and 5. Using the current procedure

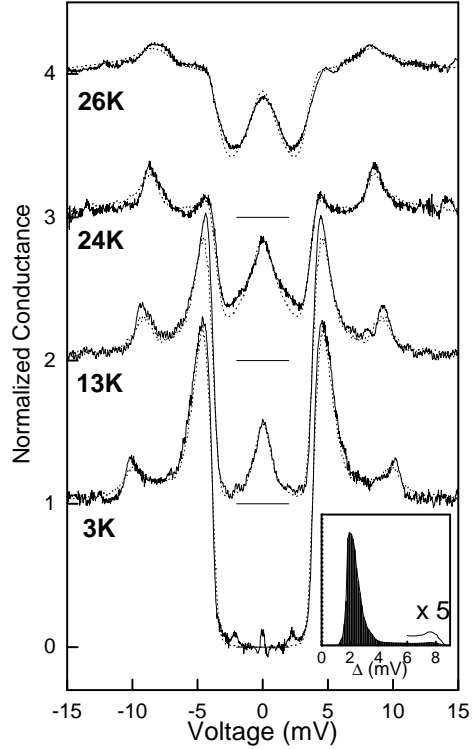


Fig. 5. The temperature dependence of the S-S spectra as measured in a junction made of two parts of single crystalline  $MgB_2$  (curves displaced by 1 in the y axis). Dashed lines are fits to these curves. For the lowest temperature curve we use a distribution of values of the superconducting gap as shown in the inset at the bottom of the figure. For higher temperatures, this distribution has to be changed slightly due to the temperature variation of the superconducting gaps. The contribution from  $\sigma$  band electrons to the tunneling current is small and leads to a broad peak, which has been zoomed out in the figure of the inset. Straight lines at the bottom of each curve indicate zero conductance for each temperature.

of taking the derivative of the conductance as a function of the bias voltage  $d(\frac{dI}{dV})/dV$  [49], which enhances the features due to the dominating gaps in the distribution, we can best identify the characteristic energy corresponding to the physical process which gives these peaks, as a maximum (minimum) in  $d(\frac{dI}{dV})/dV$  for positive (negative) voltages. The features at 3.8 and 9.5 mV are clearly due to conventional tunneling processes and are also obtained from the fit to the experimental curves shown in Figs.4 and 5. The feature in Fig.6a at 3.8mV (corresponding to the highest



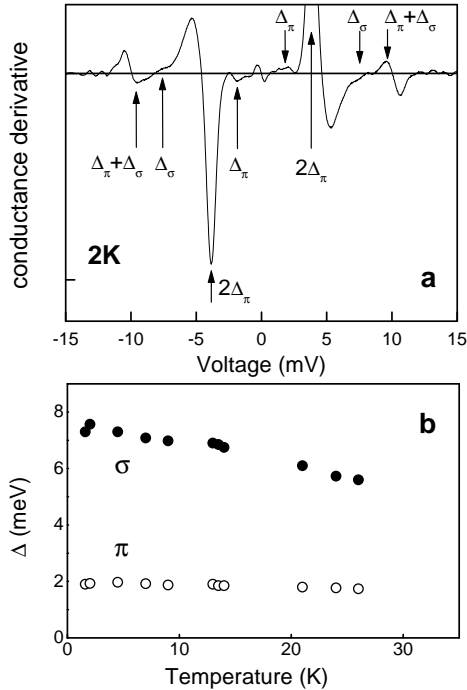


Fig. 6. The derivative of the conductance as a function of the bias voltage in the S-S junction at 2K (a). This type of plots is used to identify the voltage position of the main peaks obtained in the conductance (Figs. 4 and 5). Note that the voltage range is much larger than the one in inset of Fig.4, so that the peaks of the subharmonic gap structure of  $2\Delta_\pi$  corresponding to  $n > 2$  (located at  $2\Delta_\pi/n$ , see right bottom inset of Fig.4) appear as a very small feature at the center of this plot. The arrows show the peaks which are best identified in this voltage range. In (b) we show the temperature dependence of  $\Delta_\sigma$  and  $\Delta_\pi$  as determined by using plots as (a).

peak in Figs.4 and 5), is located at two times the dominant gap in the distribution corresponding to the  $\pi$  band gaps,  $2\Delta_\pi$ . The contribution to the tunnelling current from the  $\sigma$  band electrons is too small in these junctions to give a feature at  $2\Delta_\sigma$  as shown by the fit in Fig.5 and its associated gap distribution. The clear feature observed at 9.5mV is located at the sum of the dominant gaps of each set of bands,  $\Delta_\pi + \Delta_\sigma$ . The physical origin of this effect is that, when the bias voltage between both electrodes coincides with the sum of the peaks of both distributions  $\Delta_\pi + \Delta_\sigma$ , the high peak in the density of states corresponding to the  $\pi$  band gaps enhances the small bump corresponding to the  $\sigma$

band gaps and gives a clearly measurable peak in the conductance.

From Fig.6a we can also obtain the location of the peaks related to the subharmonic gap structure associated to the  $\Delta_\pi$  gap, already discussed in connection with Fig.4 (in Fig.6a, for clarity, we only highlight  $2\Delta_\pi/n$  with  $n = 2$ ). Interestingly, we can also observe another feature at  $\Delta_\sigma$ , possibly related to multiple Andreev reflections which enhance the conductance at the voltage corresponding to the  $n = 2$  subharmonic gap structure associated to the  $\sigma$  band gaps. This point should be analyzed in more detail by extending presently available theoretical models to multiband materials. To the best of our knowledge, no other previous measurement of this characteristic feature of S-S tunnel junctions has been made in multigap superconductors.

By using the same plot for higher temperature curves, we can also easily obtain the temperature dependence of the dominant superconducting gap features at the  $\pi$  and  $\sigma$  bands. The result is represented in Fig.6b. Note that, while  $\Delta_\pi$  stays fairly constant,  $\Delta_\sigma$  changes more rapidly as a function of temperature.

#### 4. Conclusion

We have presented new results on Scanning Tunneling Spectroscopy in single crystals and grains of  $\text{MgB}_2$ . The tunneling spectra clearly reflect the multiband character of superconductivity in this material, and are well fitted by two band BCS expressions. We mostly find features associated to the  $\pi$  band gap, which clearly dominates the contribution to the tunneling spectra, although features due to the  $\sigma$  band gaps were also detected. Both bands have a non negligible distribution of values of the superconducting gap, in agreement with the recent theoretical calculations of [31].

In some locations of the surface we can observe interesting effects with which we can extend our present understanding of this material. Interband scattering effects lead to the observation of a sin-

gle gap structure. S-S junctions show clearly the Josephson effect and the appearance of peaks at sub-multiples of the superconducting gap characteristic of this type of junctions (subharmonic gap structure).

Clearly, many questions remain open which need to be addressed in future experiments. The observation of atomic resolution images of the surface is necessary to understand the dominant role of the  $\pi$  band gap in our measurements. It is indeed striking that other important experiments, as e.g. NMR or Raman scattering [25,51], preferentially observe features associated to the  $\sigma$  band gap. In NMR [51], even no trace of the  $\pi$  band gap has been measured. Although these last experiments were made at a relatively high magnetic field (1T), which could have influenced in some way the  $\pi$  band gap, the reasons for the observation of one or the other gap structure in different experiments needs to be addressed. Furthermore, the search for phonon features in the electronic tunneling density of states in order to obtain more information about the pairing interaction is an open issue. It should also be interesting to study in more detail S-S junctions of this material in a situation with a larger contribution from the  $\sigma$  band electrons, as for instance the one presented in fig.2b, to the tunneling current to search for new features in the subharmonic gap structure and in the Josephson effect. The resulting curves should be highly non linear, opening the way to new interesting applications.

Theoretical calculations pointing out possible new phenomena to be observed in N-S and S-S tunneling experiments associated to the multigap nature of superconductivity in this compound would be very stimulating. In any case, MgB<sub>2</sub> is clearly a very intriguing superconductor with a remarkably simple Fermi surface and high critical temperature. This has made, and will continue to make, feedback between theory and experiment especially fruitful. We can therefore expect new and surprising physics to emerge from this interaction in the following years.

**Acknowledgement** We specially acknowledge F. Guinea and E. Bascones for very fruitful discussions. We also acknowledge J. Ramirez, N. Agrait and J.L. Martinez. Support from the ESF programme Vortex Matter in Superconductors at Extreme Scales and Conditions (VORTEX), as well as from MCyT (MAT2001-1281-c02-01, Spain), the Comunidad Autónoma de Madrid (Spain) and the European Social Fund is acknowledged. The single crystals of MgB<sub>2</sub> were prepared in support by the New Energy and Industrial Technology Development Organization (NEDO) as Collaborative Research and Development of Fundamental Technologies for Superconductivity Applications.

## References

- [1] J. Nagamatsu, N. Nakagawa, T. Muranaka, Y. Zenitani, J. Akimitsu, *Nature (London)*, **410**, 63 (2001).
- [2] S.L. Bud'ko, G. Lapertot, C. Petrovic, C.E. Cunningham, N. Anderson, P.C. Canfield, *Phys. Rev. Lett.* **86**, 1877 (2001).
- [3] G. Rubio-Bollinger, H. Suderow, S. Vieira, *Phys. Rev. Lett.* **86**, 5582 (2001).
- [4] A. Y. Liu, I. I. Mazin, and J. Kortus *Phys. Rev. Lett.* **87**, 087005 (2001)
- [5] E. Bascones and F. Guinea, *Phys. Rev. B* **65**, 174505 (2002)
- [6] G. Karapetrov, M. Iavarone, W. K. Kwok, G. W. Crabtree, and D. G. Hinks *Phys. Rev. Lett.* **86**, 4374-4377 (2001)
- [7] H. Schmidt, J. F. Zasadzinski, K. E. Gray, and D. G. Hinks *Phys. Rev. B* **63**, 220504 (2001)
- [8] A. Sharoni, I. Felner, and O. Millo, *Phys. Rev. B* **63**, 220508(R) (2001)
- [9] H. Suhl, B.T. Matthias and L.R. Walker, *Phys. Rev. Lett.*, **3**, 552 (1959)
- [10] G. Binnig, A. Baratoff, H. E. Hoening, and J. G. Bednorz *Phys. Rev. Lett.* **45**, 1352-1355 (1980)
- [11] C.C. Sung, V.K. Wong, *J. Phys. Chem. Solids*, **28**, 1933 (1967).
- [12] A. A. Golubov and I. I. Mazin, *Phys. Rev. B* **55**, 15146-15152 (1997)

- [13] I. I. Mazin, O. K. Andersen, O. Jepsen, O. V. Dolgov, J. Kortus, A. A. Golubov, A. B. Kuz'menko, D. van der Marel, *cond-mat/0204013*
- [14] H. Schmidt, J. F. Zasadzinski, K. E. Gray, and D. G. Hinks *Phys. Rev. Lett.* **88**, 127002 (2002)
- [15] M. Iavarone, G. Karapetrov, A. E. Koshelev, W. K. Kwok, G. W. Crabtree, D. G. Hinks, *cond-mat/0203329*.
- [16] F. Giubileo, D. Roditchev, W. Sacks, R. Lamy, D. X. Thanh, J. Klein, S. Miraglia, D. Fruchart, J. Marcus, and Ph. Monod *Phys. Rev. Lett.* **87**, 177008 (2001)
- [17] M. H. Badr, M. Freamat, Yu. Sushko, and K.-W. Ng *Phys. Rev. B* **65**, 184516 (2002)
- [18] M. R. Eskildsen, M. Kugler, S. Tanaka, J. Jun, S. M. Kazakov, J. Karpinski, O. Fischer, *cond-mat/0207394*.
- [19] P. Szabo, P. Samuely, J. Kacmarck, T. Klein, J. Marcus, D. Fruchart, S. Miraglia, C. Marcenat, and A. G. M. Jansen *Phys. Rev. Lett.* **87**, 137005 (2001)
- [20] Yu.G. Naidyuk, I.K. Yanson, L.V. Tyutrina, N.L. Bobrov, P.V. Chubov, W.N. Kang, Hyeong-Jin Kim, Eun-Mi Choi, Sung-Ik Lee, *cond-mat/0112452*.
- [21] F. Bouquet, R. A. Fisher, N. E. Phillips, D. G. Hinks, and J. D. Jorgensen *Phys. Rev. Lett.* **87**, 047001 (2001)
- [22] H. D. Yang, J.-Y. Lin, H. H. Li, F. H. Hsu, C. J. Liu, S.-C. Li, R.-C. Yu, and C.-Q. Jin, *Rev. Lett.* **87**, 167003 (2001)
- [23] Y. Wang, T. Plackowski, A. Junod, *Physica C*, **355**, 179 (2001).
- [24] F. Manzano, A. Carrington, N.E. Hussey, S. Lee and A. Yamamoto, *Phys. Rev. Lett.* **88**, 047002 (2002)
- [25] J. W. Quilty, S. Lee, A. Yamamoto, and S. Tajima, *Phys. Rev. Lett.* **88**, 087001 (2002) and *cond-mat/0206506*.
- [26] S. Tsuda, T. Yokoya, T. Kiss, Y. Takano, K. Togano, H. Kito, H. Ihara, and S. Shin *Phys. Rev. Lett.* **87**, 177006 (2001)
- [27] D.R. Armstrong and P.G. Perkins, *J. Chem. Soc. Faraday Trans.* **275**, 12 (1979).
- [28] J. Kortus, I.I. Mazin, K.D. Belashenko, V.P. Antropov and L.L. Boyer, *Phys. Rev. Lett* **86**, 4656 (2001).
- [29] J.M. An, W.E. Pickett, *Phys. Rev. Lett* **86**, 4366 (2001).
- [30] A. Brinkman, A. A. Golubov, H. Rogalla, O. V. Dolgov, J. Kortus, Y. Kong, O. Jepsen, and O. K. Andersen *Phys. Rev. B* **65**, 180517 (2002)
- [31] H.J. Choi, D. Roundry, H. Sun, M. L. Cohen, S.G. Louie, *Nature*, **418**, 758 (2002)
- [32] E. A. Yelland, J. R. Cooper, A. Carrington, N. E. Hussey, P. J. Meeson, S. Lee, A. Yamamoto and S. Tajima, *Phys. Rev. Lett.* **88**, 217002 (2002)
- [33] I. I. Mazin and J. Kortus *Phys. Rev. B* **65**, 180510 (2002)
- [34] H. Uchiyama, K.M. Shen, S. Lee, A. Damascelli, D.H. Lu, D.L. Feng, Z.X. Shen and S. Tajima, *Phys. Rev. Lett.* **88**, 157002 (2002)
- [35] P.C. Canfield, P.L. Gammel, D.J. Bishop, *Phys. Today* (1998), **51**, pp. 40-46.
- [36] C.J. Chen, *Introduction to Scanning Tunneling Microscopy*, Oxford Series in optical and imaging sciences, Oxford University Press (1993).
- [37] S.Lee, T.Masui, H.Mori, Yu.Eltsev, A.Yamamoto, S.Tajima, *cond-mat/0207247*.
- [38] J.Karpinski, M.Angst, J.Jun, S.M.Kazakov, R.Puzniak, A.Wisniewski, J.Roos, H.Keller, A. Perucchi, L. Degiorgi, M.Eskildsen, P.Bordet, L.Vinnikov, A.Mironov, *cond-mat/0207263*.
- [39] Y. Machida, S. Sasaki, H. Fujii, M. Furuyama, I. Kakeya, K. Kadowaki, *cond-mat/0207658*.
- [40] K. Voelker, M. Sigrist, *cond-mat/0208237*.
- [41] H. Suderow, M. Crespo, P. Martinez-Samper, J.G. Rodrigo, G. Rubio-Bollinger, S. Vieira, N. Luchier, J.P. Brison, P.C. Canfield *Physica C*, **369**, 106 (2002).
- [42] H. Suderow, E. Bascones, A. Izquierdo, F. Guinea, S. Vieira, *Phys. Rev. B*, **65**, 100519 (R) (2002).
- [43] V.M. Silkin, E.V. Chulkov and P.M. Echenique, *Phys. Rev. B*, **64**, 172512 (2001).
- [44] R.C. Dynes, V. Narayanamurti, J.P. Garno, *Phys. Rev. Lett.*, **41**, p. 1509 (1978).
- [45] H.F. Hess, R.B. Robinson, J.V. Waszczak, *Phys. Rev. Lett.* **64**, p. 2711 (1990).
- [46] H. Suderow, P. Martinez-Samper, N. Luchier, J.P. Brison, S. Vieira and P.C. Canfield, *Phys. Rev. B*, **64**, R020503 (2001).
- [47] P. Martinez-Samper, H. Suderow, S. Vieira, N. Luchier, J.P. Brison, P. Lejay, S. Vieira, submitted.
- [48] Y. Wang, F. Bouquet, I. Sheikin, P. Toulemonde, B. Revaz, M. Eisterer, H. W. Weber, J. Hinderer, A. Junod, *cond-mat/0208169*.
- [49] E.L. Wolf, "Principles of Electron Tunneling Spectroscopy", Oxford University Press (1989).
- [50] Y. Zhang, D. Kynion, J. Chen, J. Clarke, D.G. Hinks, G.W. Crabtree, *Appl. Phys. Lett.*, **79**, 3995 (2001).
- [51] H. Kotegawa, K. Ishida, Y. Kitaoka, T. Muranaka, and J. Akimitsu, *Phys. Rev. Lett.* **87**, 127001 (2001) and H. Kotegawa, K. Ishida, Y. Kitaoka, T. Muranaka, N. Nakagawa, H. Takagiwa and J. Akimitsu, *Phys. Rev. B* **66**, 064516 (2002)